LETTER • OPEN ACCESS

National-scale estimation of gross forest aboveground carbon loss: a case study of the Democratic Republic of the Congo

View the article online for updates and enhancements.

National-scale estimation of gross forest aboveground carbon loss: a case study of the Democratic Republic of the Congo

A Tyukavina[1], S V Stehman[2], P V Potapov[1], S A Turubanova[1], A Baccini[3], S J Goetz[3], N T Laporte[3], R A Houghton[3] and M C Hansen[1]

[1] Department of Geographical Sciences, University of Maryland, College Park, MD 20742, USA
[2] Department of Forest and Natural Resources Management, State University of New York, Syracuse, NY 13210, USA
[3] Woods Hole Research Center, Falmouth, MA 02540, USA

E-mail: atyukav@umd.edu

Abstract

Recent advances in remote sensing enable the mapping and monitoring of carbon stocks without relying on extensive *in situ* measurements. The Democratic Republic of the Congo (DRC) is among the countries where national forest inventories (NFI) are either non-existent or out of date. Here we demonstrate a method for estimating national-scale gross forest aboveground carbon (AGC) loss and associated uncertainties using remotely sensed-derived forest cover loss and biomass carbon density data. Lidar data were used as a surrogate for NFI plot measurements to estimate carbon stocks and AGC loss based on forest type and activity data derived using time-series multispectral imagery. Specifically, DRC forest type and loss from the FACET (Forêts d'Afrique Centrale Evaluées par Télédétection) product, created using Landsat data, were related to carbon data derived from the Geoscience Laser Altimeter System (GLAS). Validation data for FACET forest area loss were created at a 30-m spatial resolution and compared to the 60-m spatial resolution FACET map. We produced two gross AGC loss estimates for the DRC for the last decade (2000–2010): a map-scale estimate (53.3 ± 9.8 Tg C yr^{-1}) accounting for whole-pixel classification errors in the 60-m resolution FACET forest cover change product, and a sub-grid estimate (72.1 ± 12.7 Tg C yr^{-1}) that took into account 60-m cells that experienced partial forest loss. Our sub-grid forest cover and AGC loss estimates, which included smaller-scale forest disturbances, exceed published assessments. Results raise the issue of scale in forest cover change mapping and validation, and subsequent impacts on remotely sensed carbon stock change estimation, particularly for smallholder dominated systems such as the DRC.

1. Introduction

The United Nations Reducing Emissions from Deforestation and forest Degradation (UN-REDD) program seeks to compensate developing countries for avoiding emissions due to likely future forest clearing and logging (Houghton 2012) through the emerging REDD+ mechanism. The success of REDD+ will be defined by confirmed reductions in rates of deforestation and forest degradation. A program requirement is the capability to accurately map and monitor changes in forest carbon by estimating gross emissions as a function of area of forest loss and density of carbon stocks within areas of forest loss.

National forest inventories (NFIs) could provide detailed and comprehensive information to produce national-scale carbon stock and change estimates. However, NFIs have not been established in many developing countries that participate in the UN-REDD program (Romijn *et al* 2012). The United Nations Food and Agriculture Organization (FAO) and the UN-REDD are working on the general guidelines for implementing multi-objective NFIs in these countries (UN-REDD 2011). Meanwhile, alternative methods of national-scale carbon stocks assessment independent of the availability of systematically collected ground-based forest inventory data are being investigated and prototyped (GOFC-GOLD 2010). Goetz *et al* (2009) provided an overview of the satellite-based methods of mapping and monitoring carbon stocks, and identified three general approaches: 'stratify and multiply' (SM), when a single carbon density value is assigned to each land cover type; 'combine and assign' (CA), extending the SM approach by adding various ancillary spatial data layers; and 'direct remote sensing' (DR) approach, aimed to derive the carbon stock estimates from machine learning algorithms based on satellite observations and other detailed spatial data coupled with field measurements. The last approach requires acquisition and processing of large volumes of data to produce a national-scale carbon stock or loss estimate. The first approach, SM, also referred to as the 'biome-average approach' (Gibbs *et al* 2007), is relatively easy to implement using a limited set of published data available at low or no cost. Although this approach is fairly generalized, in that it does not capture finer-scale spatial heterogeneity of carbon stocks, the accuracy of the estimates can be increased via data refinements and overlays with other data sets in a CA approach.

For a national-level aboveground carbon (AGC) loss assessment, SM approaches require a national-scale land cover change dataset (*activity data* in the IPCC terminology IPCC 2006) and mean AGC density estimates for each land cover type (IPCC *emission factors*, here referred to as *carbon data*). Modifying the basic IPCC equation used to calculate carbon emissions (IPCC 2006, vol 1, chapter 1.2), the equation to estimate gross AGC loss within a study region or a country is the following:

$$\text{AGC loss} = \sum_{i=1}^{n} \Delta \text{AD}_i \text{CD}_i \quad (1)$$

where ΔAD_i (*activity data*) denotes the change in the extent of a given land cover type i, and CD_i (*carbon data*) represents average vegetation carbon content per land cover type.

Carbon data that are required for the national-scale AGC loss assessments in an SM approach could be derived from field inventory data (e.g. tree DBH and height measurements) converted to aboveground biomass using allometric equations (e.g. for tropical forests—from Brown 1997 and Chave *et al* 2005) or existing databases and maps of biomass carbon density (e.g. Zheng *et al* 2013, Gibbs 2006, FAO 2010, Malhi *et al* 2006). Alternatively, biomass carbon content can be mapped using multi-source lidar and radar data that are capable to capture vertical tree canopy structure (Goetz and Dubayah 2011, Treuhaft *et al* 2009). Several regional and

global-scale carbon stock maps have been created recently using the synergy of field measurements, optical, lidar and radar remotely sensed data (Saatchi *et al* 2011, Baccini *et al* 2012). Another approach, presented here, is to calibrate lidar data using co-located field measurements (Baccini *et al* 2012). In this approach, a model is derived to convert lidar waveforms into biomass estimates. The derived model is then extrapolated to a much larger population of lidar shots, providing a biomass database for assigning carbon density values to mapped forest cover types.

For REDD+ countries, deforestation is likely to be the key category for greenhouse gas emissions estimates. A good practice for these countries is to use at least IPCC Tier two or three level assessments for this category of emissions, which implies reporting uncertainties (Maniatis and Mollicone 2010). AGC stock and loss uncertainty estimates are also crucial if these datasets are to be used as inputs to carbon cycle and biosphere models. However, published land cover change datasets that may be used as activity data often lack key accuracy assessment information (e.g. description of sampling design, original error matrix, area of each map category, etc) that would permit error-adjusted estimates of the change area (Olofsson *et al* 2013). The objectives of our analyses are: (i) to illustrate the process of activity data accuracy assessment on the national level, applicable when using already published land cover data or when creating a new data set, (ii) to integrate uncertainties from activity and carbon data in a national-level forest AGC loss estimate.

In this study, we implemented a SM ('stratify and multiply') approach for assessing gross forest AGC loss in the Democratic Republic of the Congo (DRC), where forest cover change is dominated by smallholder land use and industrial selective logging (Laporte *et al* 2007). Due to the aftermath of two civil wars, persistent political unrest and lack of infrastructure, the DRC does not collect NFI data required for ground-based estimates of AGC stock and its change. Our approach employs the best available activity and carbon data at the national scale—forest extent and loss maps derived from Landsat imagery (Potapov *et al* 2012) and AGC estimates derived from GLAS-based canopy vertical structure metrics (Baccini *et al* 2012). Results include new estimates of error-adjusted area of forest cover loss between 2000 and 2010, gross AGC loss, and associated uncertainties.

2. Data

2.1. Activity data

To estimate the area of forest loss, we used Landsat-based year 2000 forest cover and 2000–2010 forest cover loss data from the Forêts d'Afrique Centrale Evaluées par Télédétection (FACET) product, available online (ftp://congo.iluci.org/FACET/DRC/). FACET data processing and mapping methodology are described in Potapov *et al* (2012). The FACET dataset provides forest cover and gross forest cover loss for three forest types: primary humid tropical forests, defined as mature humid tropical forest with canopy cover >60%; secondary forests, defined as regrowing forest
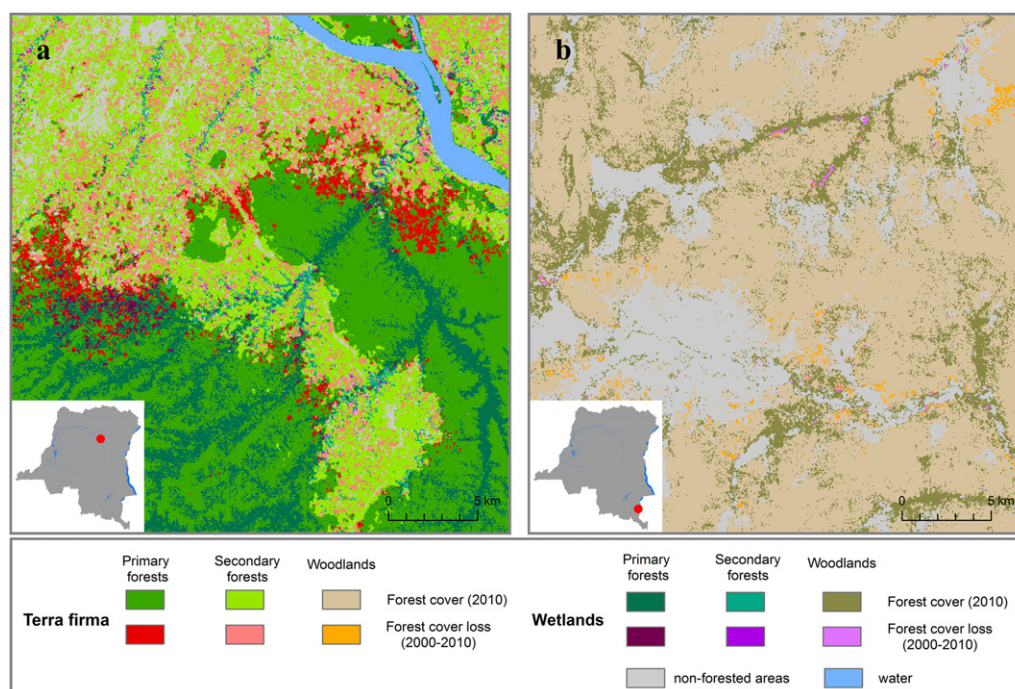
Figure 1. FACET forest cover and forest cover loss (Potapov *et al* 2012) combined with DRC wetland map (Bwangoy *et al* 2010): (a) forested area; (b) woodlands.

with canopy cover >60%; and woodlands, defined as forested areas with canopy cover 30–60%. The spatial resolution of FACET data is 60 m per pixel. We further separated these three forest types into *terra firma* (dryland) and wetland sub-classes using the DRC wetland map of Bwangoy *et al* (2010), resulting in six forest types in total. FACET forest cover loss was attributed to these new forest classes (figure 1). In this manner, the different carbon content of the antecedent forest cover could be directly related to disturbance dynamics in *terra firma* and wetland forested ecosystems. In this research, we conduct an explicit statistical validation of FACET forest cover loss for each of these forest types and derive the error-adjusted estimate of changed area based on the validation sample.

2.2. Carbon data

Mean AGC density values for each of the forest types were derived from GLAS-based biomass estimates. Baccini *et al* (2012) developed a statistical model to predict AGC densities observed in the field using GLAS lidar energy metrics in order to estimate biomass per 65 m diameter GLAS shot. The model was based on nearly 300 field sites located in 12 countries across the tropics. GLAS-predicted AGC explained 83% of variance in the field-measured carbon density at the GLAS-footprint scale with a standard error of 22.6 Mg C ha^{-1} (Baccini *et al* 2012). For this study, we employed the GLAS-derived biomass data as if they were field inventory data and did not incorporate this model uncertainty in downstream calculations. After screening GLAS data for noise and filtering for slope ($\leq 10°$), 371 458 AGC-estimated GLAS shots for the years 2004–2008 (figure 2) were analyzed

together with the combined FACET forest cover and DRC wetland maps to calculate mean AGC density values for the six target forest classes. Only shots within the forested areas that did not experience forest cover loss between 2000 and 2010 according to FACET were used for these calculations. The use of a large number of GLAS-estimated biomass values to calculate biome-average AGC densities helps avoid biases often inherent in estimates based on the compilation of point-based field measurements (i.e. paucity of sites over large areas, inadequate stratification to capture variability, and other factors that limit their spatial representativeness).

2.3. Validation data

For the purposes of activity data validation, namely the uncertainty estimation for the FACET forest cover loss, we used all available original L1T Landsat images for years 2000 and 2010 available at no charge from USGS archives (http://glovis.usgs.gov/) and annual Landsat composites for circa 2000, 2005 and 2010 (Potapov *et al* 2012). Year 2005 composite images helped identify forest cover loss in the early 2000s that might be difficult to detect in 2010 Landsat images due to rapid vegetation regeneration in the tropics.

In addition to the use of Landsat images for the validation (reference) classification, we also employed visual interpretation of very high spatial resolution images available for the study region through Google Earth^{TM} and through a partnership between NASA and NGA that provides access to unclassified commercial high spatial resolution satellite data from NGA archives for NASA Earth Science Investigators (http://cad4nasa.gsfc.nasa.gov/). A total of 1689 high resolution images from multispectral and panchromatic
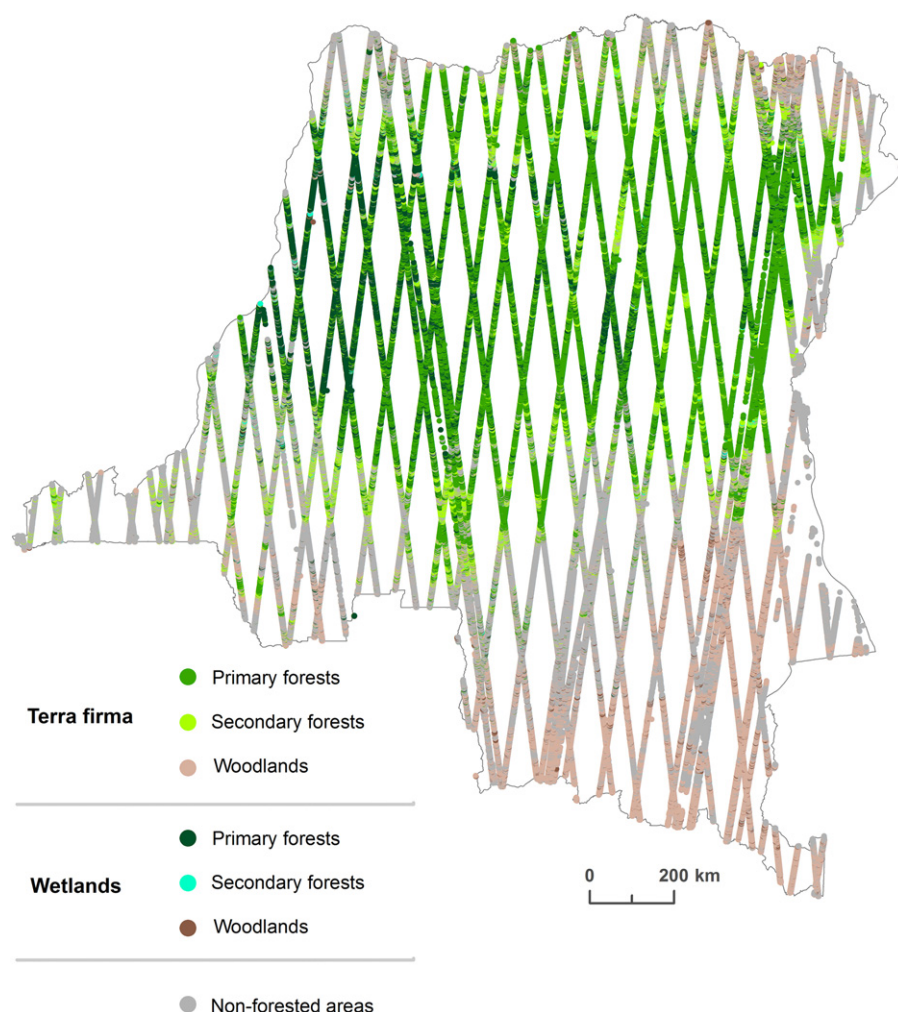
Figure 2. 2004–2008 GLAS shots color-coded by the FACET forest type (Potapov *et al* 2012) combined with wetland map (Bwangoy *et al* 2010).

sensors (Ikonos, WorldView-1, WorldView-2, Quickbird, Orbview-5) for 2008–2011 time interval were used for the visual assessment of validation samples. In total, 503 out of a final 1061 validation samples had at least one matching high resolution image available between 2000 and 2013, either from Google Earth$^{\mathrm{TM}}$ or from the NGA archive. These images facilitated the forest cover loss validation, providing information about forest cover type on date 1 (2000) or date 2 (2010).

3. Methods

3.1. Uncertainties from activity data

The key objective of activity data validation is to estimate error-adjusted area of forest cover loss for each forest type and to quantify its uncertainty. Error-adjusted area estimation uses validation sample data to adjust area of forest cover loss due to classification errors (including omission errors and excluding commission errors) present in the map product (Olofsson *et al* 2013). The choice of sampling design is determined

by this objective, as well as by feasibility issues and time constraints.

3.1.1. Sampling design and sample size. The target activity data class, forest cover loss, is relatively small compared with the unchanged forest areas; the sampling design should increase the sample representation of this rare class in order to achieve a precise estimate of forest cover loss accuracy (Khorram 1999). Moreover, our objective is forest type-specific loss area estimation and its accuracy; stratified random sampling is an appropriate choice in this case (Stehman 2009).

Initially, two strata within each forest type class were considered: 'no loss' (forests, undisturbed between 2000 and 2010) and 'loss' (2000–2010 forest cover loss). However, sufficient estimation of loss omission error within the large 'no loss' stratum requires special attention. Given a simple 'loss' and 'no loss' stratification, rates of false negatives (change omission errors) could be poorly characterized (Khorram 1999). Furthermore, the FACET national-scale forest cover loss product is likely to be conservative, i.e. omitting forest cover loss in comparison to committing

Table 1. Distribution of samples among forest types using proportional and arbitrary sample allocation strategies for stratified random sampling.

| | Proportional allocation (% samples) | | |
Forest type	Based on forest area	Based on loss area	Arbitrary allocation (% samples)
Primary forest	46	25	33
Secondary forest	11	55	17
Woodlands	21	13	25
Wetland primary forest	19	3	17
Wetland secondary forest	1	3	4
Wetland woodlands	2	1	4

forest loss. To address this issue we identified an additional 'probable loss' stratum within each forest type class. This stratum was constructed to target omitted forest cover loss in order to improve the loss area estimate for the AGC loss calculation. We define the 'probable loss' stratum as a 1-km radius circular region around forest cover loss, assuming that omission of loss is likely to occur in proximity to mapped loss. The choice of the 1-km wide 'probable loss' stratum is supported by the evidence that increased tree mortality in temperate and tropical forests is generally observed up to 1 km from the forest edge (Broadbent *et al* 2008).

A total of 18 strata were analyzed: 'loss', 'probable loss', and 'no loss' for each of the six forest types (*terra firma* and wetland primary forests, *terra firma* and wetland secondary forests, *terra firma* and wetland woodlands). Allocation of samples among these strata should effectively address our validation objective (see section 3.1) of minimizing standard errors (SEs) of error-adjusted estimators of forest cover loss area (Stehman 2012).

When considering allocation of samples among forest types, we examined both the area of forest type and the area of our target class (forest loss) within each forest type. Proportional allocation of samples among forest types based on the forest type area would lead to small sample sizes from secondary forest, woodlands and wetland forests: almost half of all samples in this case fall into the dense forest class (table 1). Although forest cover loss in dense forests that have high biodiversity and other high-value ecosystem services is important to estimate correctly, the majority of mapped forest cover loss occurred in secondary forests. However, allocation of samples based on the forest cover loss area leads to the majority of samples being located in secondary forests. In order to find a compromise between preserving a sufficient number of samples in the strategically important dense forest class while adequately representing the relatively small classes with high proportional forest cover change (secondary forest, woodlands), we implemented an arbitrary allocation that was close to proportional by forest type area, but adjusted for forest loss area (table 1).

The sample size allocation to the three strata within each forest type was determined as follows. Because it is equally important for our primary validation objective (estimation of forest loss area for each forest type based on an error matrix) to account for committed and omitted loss area, we addressed the need to account for omission errors by creating the separate 'probable loss' strata within the original 'no loss' class. Therefore, when allocating samples among

Table 2. Allocation of sample size among validation strata.

Forest type	No loss	Probable loss	Loss	Total
Primary forest	200	70	63	333
Secondary forest	30	87	50	167
Woodlands	100	90	60	250
Wetland primary forest	80	30	57	167
Wetland secondary forest	15	15	12	42
Wetland woodlands	15	15	12	42

loss strata, we chose to have an allocation closer to equal, which helped to target errors of commission (Stehman 2012) among the 'no loss', 'probable loss' and 'loss' strata. A total sample size of 1000 was projected as feasible to be visually interpreted by expert analysts. We imposed the condition that a sample size greater than 50 was required for the major forest types (primary, secondary forests, woodlands, wetland primary forests), the allocation of sample size per stratum (the sampling unit is one 60-m FACET pixel) was implemented as shown in table 2.

For the chosen sample allocation we calculated SEs of the estimated area of change using hypothetical omission and commission error rates in order to confirm that the chosen allocation would not lead to inflated standard errors. We compared our arbitrary allocation to proportional among forest allocation with equal and proportional allocation among loss strata and found that the arbitrary allocation performed as well or better than the other options. The equation used to calculate SEs of the estimated area of change for each forest type is similar to equation (3) from Olofsson *et al* (2013). However, after the assignment of reference values to the samples during expert validation, we found out that the 'probable loss' stratum contributed 35% of the total variance in primary forest, 50% of the variance in secondary forest, and 20% of the variance in woodlands. Additional random samples were added to the 'probable loss' stratum of *terra firma* primary, secondary forests and woodlands (20, 30 and 10 samples respectively) in order to minimize the total SE of the loss area estimate.

3.1.2. Estimating area of forest loss and its uncertainty.
Visual interpretation of validation samples was performed at a 30-m spatial resolution, enabling map-scale and sub-grid error assessments (FACET was made at a 60 m spatial resolution
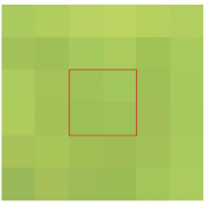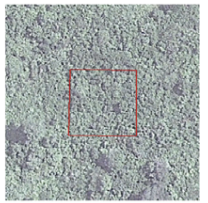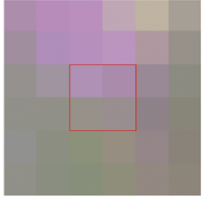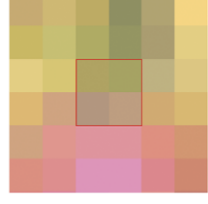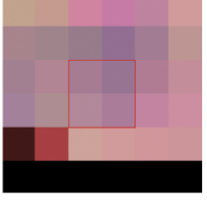
Figure 3. Example of sample block visual interpretation; for the map-scale estimate, 0.5 loss is treated as no loss. The black stripe in the 2010 Landsat loss sample is a data gap due to the Landsat 7 scan-line corrector malfunction.

Table 3. Error matrix of sample counts for map-scale and sub-grid area estimates.

| | | Reference strata | | | | |
| | | Map-scale estimate | | Sub-grid estimate | | |
Forest type	Map strata	No loss	Loss	No loss	Loss	*N* of pixels in each stratum
Primary forest	No loss	200	0	200	0	147 647 298
	No loss–probable loss	89	1	86.5	3.5	56 158 987
	Loss	3	60	3	60	2 638 342
Secondary forest	No loss	30	0	30	0	5 720 568
	No loss–probable loss	107	10	98.5	18.5	35 535 337
	Loss 00–10	3	47	3	47	5 619 034
Woodlands	No loss	100	0	100	0	51 491 436
	No loss–probable loss	98	2	97	3	39 725 284
	Loss 00–10	7	53	7	53	1 374 079
Wetland primary forest	No loss	80	0	80	0	67 675 696
	No loss–probable loss	30	0	30	0	15 706 036
	Loss 00–10	9	48	9	48	326 316
Wetland secondary forest	No loss	15	0	15	0	1 506 946
	No loss–probable loss	15	0	14.5	0.5	2 176 786
	Loss 00–10	4	8	4	8	255 498
Wetland woodlands	No loss	15	0	15	0	7 003 885
	No loss–probable loss	15	0	15	0	2 477 979
	Loss 00–10	2	10	2	10	97 176

using resampled 30-m Landsat time-series imagery). We produced two forest loss area estimates for the DRC for the last decade (2000–2010): a map-scale estimate accounting for whole-pixel classification errors in the 60-m resolution FACET forest cover change product, and a sub-grid estimate that took into account 60-m cells that experienced partial forest loss (table 3). For the map-scale estimate we treated

a 60-m validation pixel as 'loss' only if the reference forest loss fraction detected using 30-m Landsat and/or high spatial resolution was ≥75% of pixel area. For the sub-grid estimate, three gradations of reference loss fraction per pixel were used: 1 (loss) with reference loss ≥75% of pixel area; 0.5 (mixed pixels) with reference loss between 75% and 25%; and 0 (no loss) otherwise (figure 3).

Table 4. Parameters for the calculation of error-adjusted area of forest cover loss within *terra firma* primary forests (map-scale estimate).

	Primary forest					
	$\sum_{u \in h} y_u$	n_h	$\bar{y}_h$	N_h	Map area (ha)	s_{yh}^2
No loss	0	200	0/200	147 647 298	53 153 027	0.000 000 000
No loss–probable loss	1	90	1/90	56 158 987	20 217 235	0.011 111 111
Loss	60	63	60/63	2 638 342	949 803	0.046 082 949
			Total	206 444 627	74 320 066	

When the sampling strata and map classes being validated are the same, equations (2)–(4) from Olofsson *et al* (2013) should be used to calculate error-adjusted area of forest cover loss and its standard error based on a validation confusion matrix. In our case, there was a mismatch between sampling strata ('no loss', 'probable loss', 'loss') and map classes ('loss' and 'no loss') within each forest cover type arising from the attempt to target omitted forest cover loss by creating the additional 'probable loss' stratum. Based on sampling theory (Cochran 1977), the following equation was employed to produce an unbiased estimator of the area of forest cover loss within each of the forest cover types when validation strata and map classes do not match (Stehman 2013, in review):

$$\hat{A} = A_{\text{tot}} \times \frac{\sum_{h=1}^{H} N_h \bar{y}_h}{N} \quad (2)$$

where A_{tot}—total area of the forest cover type;
$y_u = 0.5$ *or* 1 if pixel *u* (or it's half) is in reference class 'forest cover loss', and $y_u = 0$ otherwise;
$\bar{y}_h = \frac{\sum_{u \in h} y_u}{n_h}$, the sample-mean of the y_u values in stratum *h*;
n_h—sample size in stratum *h*;
N_h—number of pixels in stratum *h*;
N—total number of pixels within the forest cover type.

The standard error of the error-adjusted estimate of the forest cover loss is:

$$SE(\hat{A}) = A_{\text{tot}} \sqrt{\frac{\sum_{h=1}^{H} N_h^2 \left(1 - \frac{n_h}{N_h}\right) \frac{s_{yh}^2}{n_h}}{N^2}} \quad (3)$$

where $s_{yh}^2 = \frac{\sum_{u \in h}(y_u - \bar{y}_h)^2}{n_h - 1}$, the sample variance for stratum *h*.

A 95% confidence interval (assuming normal distribution) is:

$$\hat{A} \pm 1.96 SE(\hat{A}). \quad (4)$$

An example of the forest cover loss area estimation for *terra firma* primary forests (map-scale estimate) is presented in table 4 and equations (5)–(7).

$$\hat{A} = 74\,320\,065.72(0 \times 147\,647\,298 + \tfrac{1}{90} \times 56\,158\,987$$
$$+ \tfrac{60}{63} \times 2\,638\,342)(206\,444\,627)^{-1}$$
$$= 1129\,210 \text{ ha} \quad (5)$$

$$SE(\hat{A}) = 74\,320\,065.72$$
$$\times \left[\left(147\,647\,298^2 \left(1 - \frac{200}{147\,647\,298}\right) \frac{0.0}{200} \right. \right.$$

$$+ 56\,158\,987^2 \left(1 - \frac{90}{56\,158\,987}\right) \frac{0.011\,111\,111}{90}$$

$$+ 2638\,342^2 \left(1 - \frac{63}{2638\,342}\right) \frac{0.046\,082\,949}{63} \right)$$

$$\times \; (206\,444\,627^2)^{-1} \bigg]^{1/2}$$

$$= 226\,099 \text{ ha} \quad (6)$$

$$\hat{A} = 1129\,210 \pm 443\,156 \text{ ha}. \quad (7)$$

3.2. Uncertainties from carbon data

Table 5 presents the mean and population standard deviation (STD) derived from the number of GLAS shots per forest type. Using the SM ('stratify and multiply') approach we assigned a single mean AGC density value to each of the forest type classes to estimate gross AGC loss. To quantify the uncertainty of this estimate, we employed the standard deviation of the sample-mean's estimate of a population mean, the standard error of the mean (SEM). According to the central limit theorem, the distribution of sample estimates of the mean is normally distributed, enabling us to calculate the 95% confidence interval (CI) of mean AGC density estimates as ± 1.96SEM. Table 5 shows mean AGC densities of our target forests classes along with their 95% CIs.

3.3. Combination of the uncertainties

When calculating AGC loss for each forest type using equation (1), uncertainty comes both from activity data (in our case—forest cover loss) and emission factors (carbon data). In order to combine uncertainties from these quantities, the multiplication approach from the recent IPCC Guidelines for National Greenhouse Gas Inventories (IPCC 2006, vol 1, chapter 3, p 28, equation (3.1)) was used:

$$U_{\text{total}} = \sqrt{U_1^2 + U_2^2 + \cdots + U_n^2} \quad (8)$$

where U_{total} is the percentage uncertainty in the product of the quantities (half the 95% confidence interval divided by the total and expressed as a percentage).

U_i is the percentage uncertainties associated with each of the quantities.

Table 5. GLAS-based AGC density estimates for the DRC forest types. Mean AGC densities are given with ±95% CI.

Forest type	Mean AGC density (Mg C ha^{-1})	Number of GLAS samples	STD
Primary forest	156.8 ± 0.4	115 566	67.03
Secondary forest	94.8 ± 0.7	31 443	67.45
Woodlands	71.2 ± 0.2	121 671	44.24
Wetland primary forest	128.9 ± 0.4	85 923	55.29
Wetland secondary forest	90.7 ± 2.3	3 148	65.83
Wetland woodlands	66.5 ± 0.8	13 707	45.81

Table 6. Original FACET and error-adjusted estimates of 2000–2010 forest cover loss within DRC forest types (±95% CI).

	2000–2010 forest cover loss (ha)		
	Error-adjusted		
Forest type	Map-scale estimate	Sub-grid estimate	FACET map
Primary forest	1 129 210 ± 443 156	1 690 800 ± 645 694	949 803
Secondary forest	2 994 876 ± 664 625	3 924 262 ± 736 673	2 022 852
Woodlands	722 979 ± 396 475	865 990 ± 439 210	494 668
Wetland primary forest	98 925 ± 11 218	98 925 ± 11 218	117 474
Wetland secondary forest	87 440 ± 78 014	87 441 ± 78 014	91 979
Wetland woodlands	29 153 ± 7704	29 153 ± 7704	34 983

For example, for the primary forest stratum, the calculation of the U_{total} (using the map-scale ΔAD estimate) is the following:

$$U_{\text{total}} = \sqrt{\left(\frac{\text{SE}(\hat{A})}{\hat{A}} \times 100\right)^2 + \left(\frac{\text{AGC SEM}}{\text{Mean AGC}} \times 100\right)^2}$$

$$= \sqrt{\left(\frac{226\,099.75}{1\,129\,210} \times 100\right)^2 + \left(\frac{0.2}{156.83} \times 100\right)^2}$$

$$= 20.02\%. \tag{9}$$

When calculating total gross AGC loss within the DRC (summing AGC loss values for all forest types), the addition and subtraction approach from the IPCC Guidelines (IPCC 2006, vol 1, chapter 3, p 28, equation (3.2)) was used to estimate the uncertainty of the resulting quantity:

$$U_{\text{total DRC}}$$
$$= \frac{\sqrt{(U_1 x_1)^2 + (U_2 x_2)^2 + \cdots + (U_n x_n)^2}}{|x_1 + x_2 + \cdots + x_n|} \tag{10}$$

where U_{total} is the percentage uncertainty in the sum of the quantities (half the 95% confidence interval divided by the total and expressed as percentage);

x_i and U_i are the uncertain quantities and percentage uncertainties associated with them.

Thus, the overall uncertainty of gross AGC loss estimate for the entire DRC is:

$$U_{\text{total DRC}}$$
$$= \frac{\sqrt{(U_{\text{total1}}\Delta\text{AGC}_1)^2 + (U_{\text{total2}}\Delta\text{AGC}_2)^2 + \cdots + (U_{\text{total}n}\Delta\text{AGC}_n)^2}}{|\Delta\text{AGC}_1 + \Delta\text{AGC}_2 + \cdots + \Delta\text{AGC}_n|} \tag{11}$$

where numbers (1–n) stand for the six forest cover types.

4. Results

Applying the approach of adjustment for the classification errors described in section 3, we produced estimates of forest cover loss within target DRC forest classes (table 6). Error-adjustment significantly increased estimated areas of forest loss in *terra firma* forest classes (primary, secondary forests and woodlands); omission errors prevailed over commission errors (figure 4). In the wetland forests and woodlands, on the contrary, more loss was committed in the map product; error-adjusted loss area estimates were smaller than those prior to adjustment. SE was highest in wetland secondary forests and *terra firma* woodlands. High uncertainty in the wetland secondary forests is associated with it being the smallest and spatially discontinuous class. Woodland is a challenging forest type to map and monitor due to the gradients of tree canopy cover and seasonality as well as the comparatively uneven intensity of disturbance events, all of which contributes to larger SEs.

To compare AGC density estimates for our target forest classes with published estimates, we calculated average AGC densities within the 6 DRC forest types using available spatially explicit vegetation carbon density products (Baccini *et al* 2012, Saatchi *et al* 2011, Gibbs and Brown 2007, Kindermann *et al* 2008) and compared them with the GLAS-based estimates of the current study (figure 5). This comparison provides a general understanding of how well our current estimates correspond to existing knowledge. Examination of figure 5 shows that GLAS-based AGC density estimates are generally higher than those modeled using optical remotely sensed data (Baccini *et al* 2012, Saatchi *et al* 2011, Gibbs and Brown 2007), probably because of spatial averaging (Goetz and Dubayah 2011, Zolkos *et al* 2013), but don not exceed the estimates of Kindermann *et al* (2008) who employed FAO 2005 Forest Resources Assessment statistics.
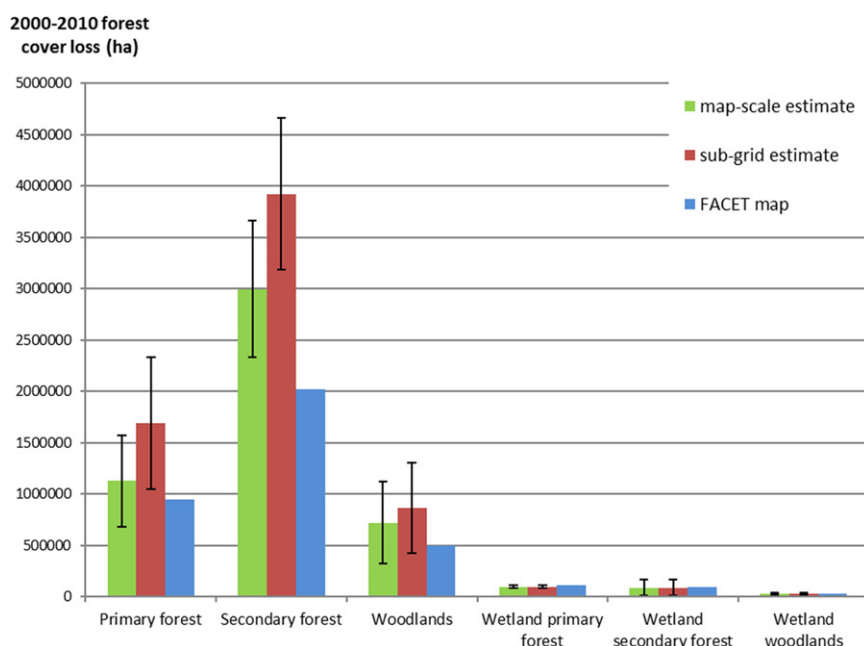
Figure 4. Forest cover loss (2000–2010) within DRC forest types; error bars are the 95% CIs.
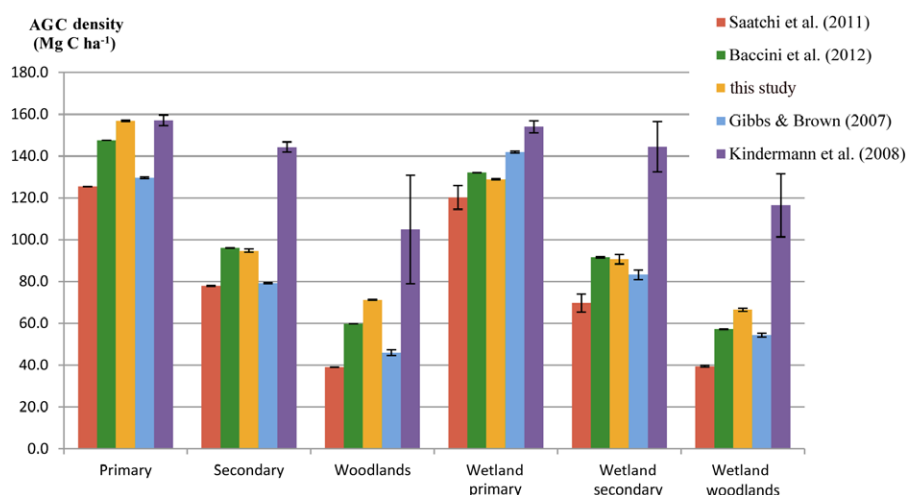

Figure 5. Comparison of the AGC density estimates from the published datasets (error bars are the 95% CIs) and the current study.

Table 7. Gross AGC loss estimates (2000–2010) with the uncertainty measures for DRC forest types (± is the 95% CI).

	Map-scale loss area estimate		Sub-grid loss area estimate	
Forest type	U_{total} (%)	Gross AGC loss 2000–2010 (Pg C)	U_{total} (%)	Gross AGC loss 2000–2010 (Pg C)
Primary forest	20.0	0.177 ± 0.070	19.5	0.265 ± 0.101
Secondary forest	11.3	0.284 ± 0.063	9.6	0.372 ± 0.070
Woodlands	28.0	0.051 ± 0.028	25.9	0.062 ± 0.031
Wetland primary forest	5.8	0.013 ± 0.001	5.8	0.013 ± 0.001
Wetland secondary forest	45.5	0.006 ± 0.005	45.5	0.008 ± 0.007
Wetland woodlands	13.5	0.002 ± 0.001	13.5	0.002 ± 0.001
DRC total	9.4	0.533 ± 0.098	9.0	0.721 ± 0.127

Sub-grid gross AGC loss estimates were 20–50% higher than map-scale ones for the major *terra firma* forests (primary, secondary forests and woodlands) and nearly equal for the less widespread wetland forests (table 7, figures 6(b) and (c)).

Differences between these estimates are mostly associated with the 'loss' and 'probable loss' strata, particularly in regions where primary and secondary forest loss predominate. There are no significant differences in the forests and
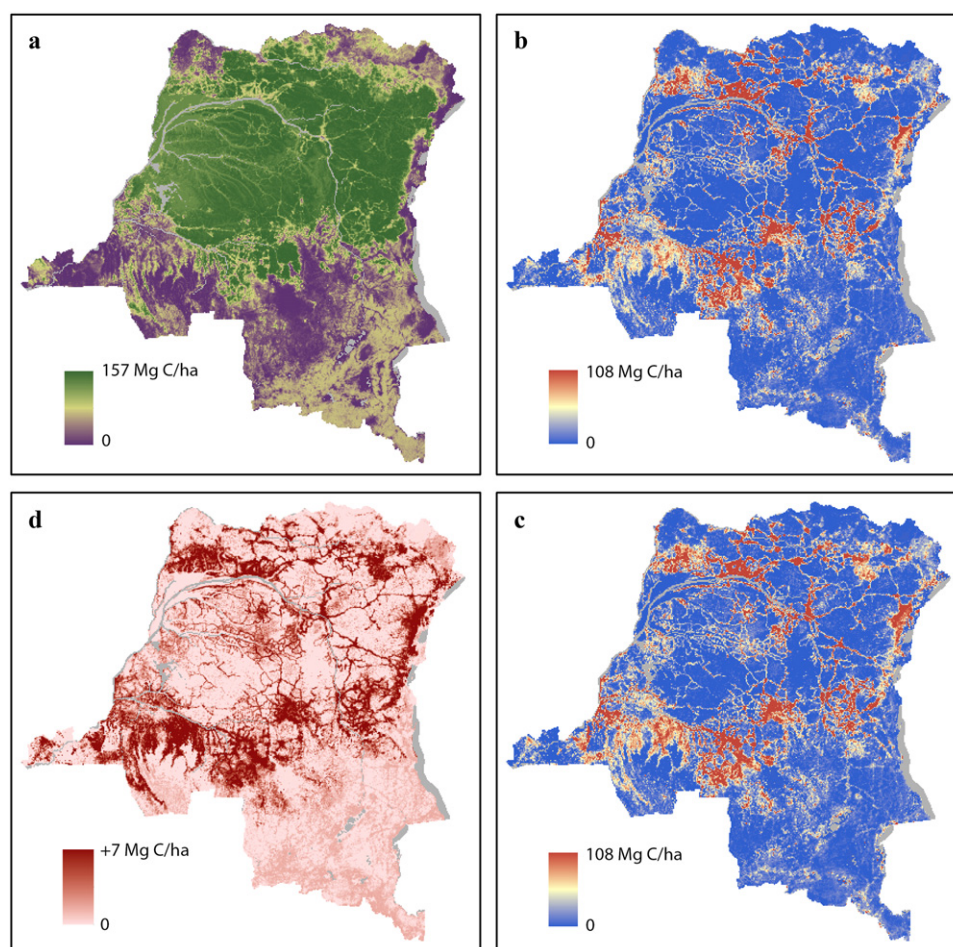
Figure 6. Forest type and strata averages, aggregated to a 5-km grid: (a) year 2000 AGC; (b) map-scale estimate of 2000–2010 gross AGC loss; (c) sub-grid estimate of 2000–2010 AGC loss; (d) difference between sub-grid and map-scale estimates. Water bodies are shown in gray. Note that AGC values for both (b) and (c) are the same for the respective forest types.

woodlands of the 'no loss' strata (figure 6(d)). For the whole of the DRC, the sub-grid AGC loss estimate was 35% higher than the map-scale estimate (table 7).

The comparison of gross forest cover loss and gross AGC rates from this study with published estimates is presented in table 8. We report annual forest cover loss rates separately for primary and secondary forests, excluding woodlands (table 8) to best match the definition of forests employed in the most recent regional sample-based forest cover loss estimate by Ernst *et al* (2013) (all tropical moist forests, excluding woodland savannahs and tropical dry forests).

5. Discussion

The results reported in table 8 need to be considered in the context of inconsistencies in methodologies, definitions, and areas of analysis (a direct consequence of the differences in the definitions of forest and woodlands). Our map-scale 2000–2010 annual forest cover loss estimate within dense forests (0.35% ± 0.03%) agrees well with the estimates of Ernst *et al* (2013) for the first half of the decade (0.32% ± 0.05%) and of Hansen *et al* (2013) for 2000–2012 (0.34%). Our map-scale estimate also falls within the

confidence interval of the global sample-based estimate of Hansen *et al* (2010), but is significantly higher than the FACET map-based estimate without error-adjustment (Potapov *et al* 2012). The sub-grid estimate, accounting for the finer-scale forest disturbance, is 30–40% higher than published estimates for the DRC, and points to the difficulty of mapping forest change in a landscape where smallholder shifting cultivation predominates. For example, FACET forest cover loss has a mean patch area of 1.4 ha (Potapov *et al* 2012). While patch size is not the same as field size, it is worth noting that typical shifting cultivation practices in the tropics employ field sizes well under 1 ha (Aweto 2013). The quantification of such change is challenging and represented by the comparatively large presence of mixed pixels in the FACET data. The difference of two methodologically consistent loss area estimates based on input data of different resolutions (60-m FACET and 30-m Hansen *et al* 2013, table 8) prior to error-adjustment illustrates the issue: the 30-m product depicts 1.5 times more change than the 60-m one. Any binary (yes/no) change map will have scale-dependent omission errors. These 'cryptic disturbances' have been reported to add more than 50% of forest cover loss

Table 8. Comparison of forest cover and carbon loss estimates for the DRC (±95% CI).

			2000–2005	2005–2010
	Source	Extent	Annual gross forest cover loss (% of the forest area)	
Current study	Map-scale	Forests + woodlands	0.32% ± 0.03%	
	Sub-grid	Forests + woodlands	0.42% ± 0.03%	
	Map-scale	Forests	0.35% ± 0.03%	
	Sub-grid	Forests	0.47% ± 0.04%	
FACET map Potapov *et al* (2012)—60 m		Forests + woodlands	0.22%	0.25%
Hansen *et al* (2013)—30 m		Forests + woodlands	0.34%	
Ernst *et al* (2013)		Forests	0.32% ± 0.05%	—
Hansen *et al* (2010)		Forests + woodlands	0.12% ± 0.23%	—
			Annual *net* forest cover loss (% of the forest area)	
FAO (2010)		Forests + woodlands	0.20%	0.20%
Ernst *et al* (2013)		Forests	0.22%	0.22%
			Annual *gross* AGC loss (Tg C yr^{-1})	
Current study	Map-scale	Forests + woodlands	53.3 ± 9.8	
	Sub-grid	Forests + woodlands	72.1 ± 12.7	
			Annual *gross* carbon loss (Tg C yr^{-1})	
Harris *et al* (2012)		Forests + woodlands	23	—

to existing Landsat-scale forest disturbance classifications for the Amazon Basin (Asner *et al* 2005).

Table 8 reflects a second type of omission error related to algorithmic and/or data limitations. Estimates of forest loss derived at a 30-m spatial resolution, particularly the Hansen *et al* (2013) and Ernst *et al* (2013) products, have comparable gross forest cover loss rates, 0.34% and 0.32% ± 0.05%. However, the 30-m validation estimate is 0.47% ± 0.04%. Large area mapping algorithms are often conservatively implemented in attempting to avoid commission error. For validation, the determination of loss/no loss is performed independently per sample and is free of this consideration. Differences between the Hansen *et al* (2013) 30-m map and the Ernst *et al* (2013) 30-m sample estimates could be due to this fact. However, the estimate of Ernst *et al* (2013) was also sample based. The additional loss found in our validation effort compared to Ernst *et al* (2013), while partially due to the use of very high spatial resolution data for a portion of the reference samples, is not easily explained and may be more related to definitional differences or other methodological factors. In summary, the difference between the 60-m FACET loss rates of 0.22% and 0.25% and the 30-m loss rates of 0.34% and 0.32% is most likely related to the differing scales of measurement. The difference between the 30-m loss rates of 0.34% and 0.32% and the validation rate of 0.47% is most likely related to limitations in mapping versus sampling or to other methodological factors. The discrepancy between map-scale and sub-grid estimates emphasizes the issue of scale in change area estimation for smallholder dominated landscapes like the DRC.

The approach for validating activity data employed in this study is relatively straightforward and easy to implement. The method allows for the generation of error-adjusted loss area estimates from the existing land cover and vegetation maps. This approach does not require large volumes of data processing and is therefore not limited by computational facilities. The use of open access medium- and high resolution imagery for map product validation (USGS Landsat archive,

Google Earth^{TM} high resolution imagery) allows defining reference values of validation samples without *in situ* measurements. Despite its advantages, the method is sensitive to sampling design and the associated decision of how to allocate the sample size among validation strata. For the strata and sample size allocation implemented in this study, the decisions were advantageous; for the four largest forest types, the reduction in standard error attributable to the stratification was substantial. Specifically, the gain in precision due to stratification can be computed from the sample data (Cochran 1977, section 5A.11) as the ratio of the standard error that would have been obtained from simple random sampling to the standard error obtained from the stratified design implemented (same sample size for both designs). For the four largest forest types, these ratios were 1.42 for primary forest, 1.10 for secondary forest, 1.32 for woodlands, and 23.21 for wetland primary forest (the latter estimate is likely inflated by the fact that two of the three strata had 0% forest loss). The methodology is also highly dependent on the knowledge base of the remote sensing experts performing visual interpretation of validation samples. Finally, it is a function of the quality of the reference imagery and the resulting clarity or conversely ambiguity in assigning change per validation sample. The map-scale and sub-grid estimates reflect the importance of this issue.

A further consideration in assessing the results concerns the reference data and the potential volatility of the sample-based estimate itself. Table 4 illustrates this issue. The 'loss' stratum records 60 of 63 samples as having experienced *terra firma* primary forest cover loss, representing 905 574 ha of error-adjusted forest loss area. For the 'probable loss' stratum, 1 of 90 samples was interpreted as having experienced forest cover loss. Due to the much larger size of this stratum, this one sample accounts for an estimated 224 635 ha of error-adjusted forest loss area, or fully 20% of *terra firma* primary forest cover loss. Without the use of the 'probable loss' stratum and the inclusion of this single sample of commission error, results would indicate a slight underestimate of *terra firma*

forest cover loss. Validation studies should formally consider likely regions of false negatives of forest change in developing stratified sampling methods for error-adjusted area estimation. The validity of the sample-based estimate is a function of many factors, including the vagaries of any individual sample data set used in creating the error-adjusted estimates.

Estimates of carbon density derived using different methods can vary considerably within the same region (Houghton *et al* 2001), introducing uncertainty to the carbon loss estimation. However, recent published estimates of carbon loss from deforestation differ primarily due to major disagreements in the quantification of the areal extent of forest cover loss (Pan *et al* 2011, Harris *et al* 2012). The DRC gross AGC loss estimates from the current study (map-scale and sub-grid) are 2 to 3 times higher than the biomass carbon loss (total carbon, above- and belowground) estimate of Harris *et al* (2012) (table 8) due primarily to differences in the estimated area of forest cover loss. The Harris *et al* (2012) estimate is based on a global forest cover loss product by Hansen *et al* (2010) that is highly uncertain in the DRC (SE = 100%, see table 8). Hansen *et al* (2010) employed a pan-tropical MODIS-based stratification to target sample allocation with only 7 samples located in the DRC. The small sample size resulted in a high standard error (table 8). Harris *et al* (2012) reported a 90% carbon loss prediction interval for the DRC, based on a Monte Carlo approach: 16–32 Tg C yr^{-1}; our current DRC gross AGC loss estimates, map-scale (53.3 Tg C yr^{-1}) and sub-grid (72.1 Tg C yr^{-1}), are not within this interval.

In our analysis, DRC gross forest AGC loss assessment consists only of stand-replacement forest disturbance that can be observed at the mapping scale and in reference data. However, forest degradation processes that do not lead to the complete loss of tree canopy or cause small-scale canopy openings, and can be detected only in the field or using dense series of sub-meter remotely sensed data may result in significant AGC loss at the national scale (IPCC 2003, Schoene *et al* 2007). One possible approach to assess the loss of biomass from these disturbances could be based on monitoring changes in the area of intact forest landscapes (Potapov *et al* 2008) and assigning an AGC loss value to the forests that have undergone the transition from intact primary to primary degraded and secondary forests (Margono *et al* 2012, Zhuravleva *et al* 2013). For countries such as the DRC, where large-scale agro-industrial forest disturbance is largely absent, the question of scale and its impact on AGC loss due to deforestation and degradation remains an important line of scientific inquiry.

We employed GLAS-based AGC estimates as a proxy for the ground-based NFI data. There are some known issues and limitations concerning the estimation of biomass from GLAS metrics. For example, GLAS-estimated vegetation heights often used in AGC models have on average 2–3-m error when compared with USDA Forest Inventory and Analysis (FIA) and other field-measured heights (Pflugmacher *et al* 2008, Lefsky *et al* 2005, Sun *et al* 2008). GLAS-derived biomass estimates are also known to be affected by the season of data acquisition and terrain slope (Sun *et al*

2008). In total, GLAS-based AGC models explain from 73% (Lefsky *et al* 2005, Pflugmacher *et al* 2008) to 83% (current study; Baccini *et al* 2012) of the variance in field-estimated biomass. Regional forest inventory data are required to calibrate and validate the current forest type GLAS-based estimates. Additional field data collection could further refine the estimates but, unfortunately, GLAS observations are not available after 2009, posing a near-term challenge for improved AGC mapping and monitoring beyond the current models. As part of the process of establishing an NFI for the DRC continues, other sources of remotely sensed data characterizing vegetation vertical structure, such as airborne lidar or spaceborne radar data, can bridge the gap until systematic spaceborne lidar measurements become available to the scientific and REDD+ implementation communities.

6. Conclusion

We applied a method of error-adjustment of forest cover loss area to produce a national-scale gross forest AGC loss estimate for the DRC based on a published forest cover loss dataset. We employed field-calibrated GLAS lidar-derived biomass carbon densities as a substitute for NFI data, which do not exist for the territory of the DRC. Two realizations of the resulting DRC gross AGC loss estimate, map-scale and sub-grid, were produced. The sub-grid AGC loss estimate accounted for disturbances finer than the map grid scale of 60 m and was higher than published estimates, highlighting issues of scale and spatial averaging in AGC estimation. Omitted disturbances were largely related to smallholder agriculture land cover change, the detection of which is scale-dependent. For the FACET product, the input Landsat imagery were averaged to 60 m and then classified, leading to the estimated scale-related omission error. Other processing steps can lead to change omission, either through the algorithm itself, for example image segmentation, post-processing of the output classification, or the application of a minimum mapping unit. In Brazil, where agro-industrial land conversion results in large forest disturbances, the Brazilian Space Agency's PRODES product 6.25 ha minimum mapping unit (the equivalent of approximately 69 Landsat pixels) (INPE 2012), provides a viable deforestation monitoring approach. However, a 6.25 ha minimum mapping unit for the DRC would omit the majority of change. For heterogeneous landscapes with change dynamics at or finer than the resolution of Landsat data, higher spatial resolution imagery to directly map such changes, or indirect methods to delimit degraded areas and subsequently relate to *in situ* measurements, are required.

Our study also illustrates the importance of reference forest state in assessing carbon dynamics, as with the primary, secondary and woodland forest types presented here. The Brazilian PRODES product, the current standard for national-scale forest monitoring, quantifies only the loss of primary forest in the Legal Amazon. While reducing primary humid tropical forest loss is the main focus of climate mitigation strategies such as REDD+, other forest types and even trees outside of forests will be part of national carbon

accounting schemes. Our study underscored the importance of monitoring other forest dynamics, as we found AGC loss in secondary forests to be 140% that of primary forests. The reuse of secondary forests remains a challenge to carbon monitoring and the development of appropriate strategies for reducing emissions, but monitoring all relevant forest types and dynamics is required as national-scale programs are developed and implemented.

REDD+ mechanisms will rely on accurate mapping and monitoring of AGC (Houghton *et al* 2010). However, scientific, technical and operational aspects of AGC mapping and monitoring are still in their infancy. Results from this study have significant implications for policy initiatives like REDD+. It is clear that the spatial scale of forest change characterization, reference information on forest type and carbon stock, and sample representativeness, can all dramatically impact AGC loss estimation. For example, considering change at a 30 m validation scale, an extra 35% of AGC loss was estimated compared to the 60-m spatial scale; *terra firma* secondary forest cover loss accounted for 40% more AGC loss than that of *terra firma* primary forest loss; a single validation sample added 20% to map-scale *terra firma* primary forest cover loss area. The volatility of results within this study indicates the DRC to be a challenging environment for quantifying changes to forest carbon stocks, with implications for other countries as well. Eventual national monitoring systems will need to demonstrate spatio-temporal consistency given the various factors that impact AGC loss estimation. While absolute accuracies may differ due to some of the aforementioned factors, relative consistency for any particular set of observations and spatial scale should be achievable and implementable. Demonstrating such consistency will be a proof of readiness for REDD+ monitoring.

Acknowledgments

References

Asner G P, Knapp D E, Broadbent E N, Oliveira P J C, Keller M and Silva J N 2005 Selective logging in the Brazilian Amazon *Science* **310** 480–2

Aweto A O 2013 *Shifting Cultivation and Secondary Succession in the Tropics* (Wallingford, UK: CABI)

Baccini A *et al* 2012 Estimated carbon dioxide emissions from tropical deforestation improved by carbon-density maps *Nature Clim. Change* **2** 182–5

Broadbent E, Asner G, Keller M, Knapp D, Oliveira P and Silva J 2008 Forest fragmentation and edge effects from deforestation and selective logging in the Brazilian Amazon *Biol. Conserv.* **141** 1745–57

Brown S 1997 Estimating biomass and biomass change of tropical forests: a primer *FAO Forestry Paper 134* (Rome: Food and Agriculture Organisation of the UN)

Bwangoy J B, Hansen M C, Roy D P, Grandi G De and Justice C O 2010 Wetland mapping in the Congo Basin using optical and radar remotely sensed data and derived topographical indices *Remote Sens. Environ.* **114** 73–86

Chave J *et al* 2005 Tree allometry and improved estimation of carbon stocks and balance in tropical forests *Oecologia* **145** 87–99

Cochran W G 1977 *Sampling Techniques* (New York: Wiley)

Ernst C, Mayaux P, Verhegghen A, Bodart C, Christophe M and Defourny P 2013 National forest cover change in Congo Basin: deforestation, reforestation, degradation and regeneration for the years 1990, 2000 and 2005 *Glob. Change Biol.* **19** 1173–87

FAO 2010 Global forest resources assessment 2010 *FAO Forestry Paper 163* (Rome: Food and Agriculture Organization of the UN)

Gibbs H K 2006 *Major World Ecosytem Complexes Ranked by Carbon in Live Vegetation: An Updated Database Using the GLC2000 Land Cover Product* NDP-017b

Gibbs H K and Brown S 2007 Geographical distribution of woody biomass carbon in tropical africa: an updated database for 2000 NDP-055b

Gibbs H K, Brown S, Niles J O and Foley J A 2007 Monitoring and estimating tropical forest carbon stocks: making REDD a reality *Environ. Res. Lett.* **2** 045023

Goetz S J, Baccini A, Laporte N T, Johns T, Walker W, Kellndorfer J, Houghton R A and Sun M 2009 Mapping and monitoring carbon stocks with satellite observations: a comparison of methods *Carbon Balance Manag.* **4** 2

Goetz S J and Dubayah R 2011 Advances in remote sensing technology and implications for measuring and monitoring forest carbon stocks and change *Carbon Manag.* **2** 231–44

GOFC-GOLD 2010 A sourcebook of methods and procedures for monitoring and reporting anthropogenic greenhouse gas emissions and removals caused by deforestation, gains and losses of carbon stocks in forests remaining forests, and forestation *Report Version* COP16-1 (Alberta: GOFC-GOLD Project Office, Natural Resources Canada)

Hansen M C *et al* 2013 The first high-resolution global maps of 21st century forest cover change at press

Hansen M C, Stehman S V and Potapov P V 2010 Quantification of global gross forest cover loss *Proc. Natl Acad. Sci.* **107** 8650–5

Harris N L, Brown S, Hagen S C, Saatchi S S, Petrova S, Salas W, Hansen M C, Potapov P V and Lotsch A 2012 Baseline map of carbon emissions from deforestation in tropical regions *Science* **336** 1573–6

Houghton R A 2012 Carbon emissions and the drivers of deforestation and forest degradation in the tropics *Curr. Opin. Environ. Sustain.* **4** 597–603

Houghton R A, Greenglass N, Baccini A, Cattaneo A, Goetz S, Kellndorfer J, Laporte N and Walker W 2010 The role of science in reducing emissions from deforestation and forest degradation (REDD) *Carbon Manag.* **1** 253–9

Houghton R A, Lawrence K T, Hackler J L and Brown S 2001 The spatial distribution of forest biomass in the Brazilian Amazon: a comparison of estimates *Glob. Change Biol.* **7** 731–46

Instituto Nacional de Pesquisas Especias 2012 *Monitoring of the Brazilian Amazonian Forest by Satellite, 2000–2012*

IPCC 2003 *Definitions and Methodological Options to Inventory Emissions from Direct Human-induced Degradation of Forests and Devegetation of Other Vegetation Types* (Hayama, Japan: The Institute for Global Environmental Strategies)

IPCC 2006 *2006 IPCC Guidelines for National Greenhouse Gas Inventories* ed H S Eggleston, L Buendia, K Miwa, T Ngara and K Tanabe (Hayama, Japan: IGES)

Khorram S 1999 *Accuracy Assessment of Remote Sensing-Derived Change Detection* ed S Khorram (Bethesda, MD: American Society for Photogrammetry and Remote Sensing)

Kindermann G E, Mccallum I, Fritz S and Obersteiner M 2008 A global forest growing stock, biomass and carbon map based on FAO statistics *Silva Fenn.* **42** 387–96

Laporte N T, Stabach J A, Grosch R, Lin T S and Goetz S J 2007 Expansion of industrial logging in central Africa *Science* **316** 1451

Lefsky M A, Harding D J, Keller M, Cohen W B, Carabajal C C, Espirito-Santo F D B, Hunter M O and de Olivera R Jr 2005 Estimates of forest canopy height and aboveground biomass using ICESat *Geog. Res. Lett.* **32** L22S02

Malhi Y *et al* 2006 The regional variation of aboveground live biomass in old-growth Amazonian forests *Glob. Change Biol.* **12** 1107–38

Maniatis D and Mollicone D 2010 Options for sampling and stratification for national forest inventories to implement REDD + under the UNFCCC *Carbon Balance Manag.* **5** 9

Margono B A, Turubanova S, Zhuravleva I, Potapov P, Tyukavina A, Baccini A, Goetz S and Hansen M C 2012 Mapping and monitoring deforestation and forest degradation in Sumatra (Indonesia) using Landsat time series data sets from 1990 to 2010 *Environ. Res. Lett.* **7** 034010

Olofsson P, Foody G M, Stehman S V and Woodcock C E 2013 Making better use of accuracy data in land change studies: estimating accuracy and area and quantifying uncertainty using stratified estimation *Remote Sens. Environ.* **129** 122–31

Pan Y *et al* 2011 A large and persistent carbon sink in the world's forests *Science* **333** 988–93

Pflugmacher D, Cohen W, Kennedy R and Lefsky M 2008 Regional applicability of forest height and aboveground biomass models for the Geoscience Laser Altimeter System *Forest Sci.* **54** 647–57

Potapov P V, Turubanova S A, Hansen M C, Adusei B, Broich M, Altstatt A, Mane L and Justice C O 2012 Quantifying forest cover loss in democratic republic of the Congo, 2000–2010, with Landsat ETM + data *Remote Sens. Environ.* **122** 106–16

Potapov P V *et al* 2008 Mapping the world's intact forest landscapes by remote sensing *Ecol. Soc.* **13** 51

Romijn E, Herold M, Kooistra L, Murdiyarso D and Verchot L 2012 Assessing capacities of non-Annex I countries for national forest monitoring in the context of REDD + *Environ. Sci. Policy* **19–20** 33–48

Saatchi S S, Harris N L, Brown S, Lefsky M, Mitchard E T A and Salas W 2011 Benchmark map of forest carbon stocks in tropical regions across three continents *Proc. Natl Acad. Sci.* **108** 9899–904

Schoene D, Killmann W, Von Luepke H and LoycheWilkie M 2007 Definitional issues related to reducing emissions from deforestation in developing countries *Forest and Climate Change Working Paper 5* (Rome: Food and Agriculture Organization of the UN)

Stehman S V 2009 Sampling designs for accuracy assessment of land cover *Int. J. Remote Sens.* **30** 5243–72

Stehman S V 2012 Impact of sample size allocation when using stratified random sampling to estimate accuracy and area of land-cover change *Remote Sens. Lett.* **3** 111–20

Stehman S V 2013 Estimating area and map accuracy for stratified random sampling when the strata are different from the map classes *Int. J. Remote Sens.* in review

Sun G, Ranson K, Kimes D, Blair J and Kovacs K 2008 Forest vertical structure from GLAS: an evaluation using LVIS and SRTM data *Remote Sens. Environ.* **112** 107–17

Treuhaft R N, Chapman B D, Dos Santos J R, Gonçalves F G, Dutra L V, Graça P M L A and Drake J B 2009 Vegetation profiles in tropical forests from multibaseline interferometric synthetic aperture radar, field, and lidar measurements *J. Geophys. Res.* **114** D23110

UN-REDD 2011 Expert meeting on assessment of forest inventory approaches for REDD + *Meeting Report* (Rome: UN-REDD Programme)

Zheng D L, Prince S D and Wright R 2013 *NPP Multi-Biome: Gridded Estimates for Selected Regions Worldwide, 1954–1998, R3. Data set* (Oak Ridge, TN: Oak Ridge National Laboratory Distributed Active Archive Center)

Zhuravleva I, Turubanova S, Potapov P, Hansen M, Tyukavina A, Minnemeyer S, Laporte N, Goetz S, Verbelen F and Thies C 2013 Satellite-based primary forest degradation assessment in the Democratic Republic of the Congo, 2000–2010 *Environ. Res. Lett.* **8** 024034

Zolkos S G, Goetz S J and Dubayah R 2013 A meta-analysis of terrestrial aboveground biomass estimation using lidar remote sensing *Remote Sens. Environ.* **128** 289–98